SMEI EM Camera Thermal Balance Test Report

C.J. Eyles

S.M. Mahmoud

C.V. Goodall

I.G. Butler

University of Birmingham

Issue 1

25 Jan 2000

Table of Contents

SMEI EM Camera Thermal Balance Test Report

1. Introduction

The report describes the thermal balance tests carried out on the SMEI Engineering Model Camera using the Birmingham thermal vacuum test facility during October 1999. The main objective of the tests was to characterise the thermal behaviour of the Camera and to derive a correlated thermal model which has now been delivered to Spectrum Astro Inc for incorporation into an integrated thermal model of the whole spacecraft. Important parameters which were determined are:

- Thermal conductances along the baffle stack and between the baffle stack and the Strong-Box.
- Parasitic thermal load on the CCD-Coldfinger assembly.
- Preliminary values for the heater power input required at the Strong-Box to spacecraft interface in Survival and Operating Modes.

The tests provided only limited data regarding the in-orbit thermal performance of the instrument since this depends significantly on the local spacecraft environment, together with solar UV and Earth IR inputs, which were not simulated in the tests.

2. Description of the Hardware

The SMEI Cameras comprise three major components – the Baffle assembly, the Strong-Box and the E-Box. The Engineering Model unit, which has now undergone qualification-level vibration tests, thermal vacuum tests and thermal balance tests, is identical to the flight units except in the following respects:

- In the EM the Radiator views along the optical axis of the instrument ($+Z_C$ direction). The orientations of the CCD Radiators on the FM units is still TBD but are unlikely to be in the same orientation as the EM.
- The Mirrors M1 and M2 are replaced by mass dummies, which should also have similar thermal properties to the flight mirrors.
- The aperture Door has been re-designed in minor respects for the FM in order to increase its mechanical stiffness.
- The power dissipation in the E-Box has increased from 5.0W for the EM to 6.3W for the FM, due to design changes on the power conversion PCB.

For the purpose of the thermal balance tests the following changes were made to the configuration of the EM Camera:

- Owing to the limited height available in the thermal balance chamber and the configuration of the LN2 Radiator, the "flight-like" CCD Radiator on the Camera had to be removed and replaced by a radiator of a similar area (400 cm^2) which lay flat over the top of the Strong-Box (see Figure 1).
- Also due to the limited space in the chamber, the Door was removed completely for "Door Open" case tests. It is believed that this did not significantly affect results since the thermal coupling between the Door and Baffle is very low given the isolation provided by the door hinges. For "Door Closed" case tests the Door was fitted (in the closed position).

- A dummy CCD package was bonded to the Coldfinger and connected by ribbon cables to the preamplifier PCB in the E-Box, thereby ensuring that the thermal characteristics were representative of the flight units.
- Initially, the EM E-Box was fitted. However, for the last five of the eighteen test cases it was replaced by a representative mass dummy which had identical mechanical and thermal interfaces to the Strong-Box and had heaters to simulate the 6.3W dissipation of the FM Cameras.

3. Description of the SMEI Camera Thermal Model

The SMEI Camera has been modelled as a thermal network (i.e. lumped parameter method) using ESATAN/THERMICA software. The SMEI Camera thermal model comprises 26 thermal nodes as listed in Table 1. Diagrams showing the geometrical configuration of the nodes are given in Appendix 1.

Node No	Description
1	Baffle rear section bottom ($-Y_C$)
2	Baffle middle section bottom ($-Y_C$)
3	Baffle front section bottom ($-Y_C$)
4	Baffle rear section top ($+Y_C$)
5	Baffle middle section top ($+Y_C$)
6	Baffle front section top ($+Y_C$)
7	Baffle rear section side ($+X_C$)
8	Baffle middle section side ($+X_C$)
9	Baffle front section side ($+X_C$)
10	Baffle rear section side ($-X_C$)
11	Baffle middle section side ($-X_C$)
12	Baffle front section side ($-X_C$)
13	Strong-Box front ($+Z_C$)
14	Strong-Box top ($+Y_C$)
15	Strong-Box bottom ($-Y_C$)
16	Strong-Box rear ($-Z_C$)
17	Strong-Box side ($+X_C$)
18	Strong-Box side ($-X_C$)
19	E-Box top ($+Y_C$)
20	E-Box bottom ($-Y_C$)
21	E-Box rear ($-Z_C$)
22	E-Box side ($+X_C$)
23	E-Box side ($-X_C$)
24	Door – *not applicable to thermal balance test*
25	Spacecraft I/F Plate – Boundary node
26	CCD Radiator – Boundary node

Table 1 - SMEI Camera Thermal Nodes

The various components of the camera are modelled as follows:

- The Baffle is divided into 3 sections along its length, with each section having 4 nodes corresponding to the 4 sides of the Baffle assembly, giving a total of 12 nodes. This is obviously a simplification given that the Baffle stack actually consists of 8 sections but it was regarded as a reasonable compromise between complexity of the model and the need to represent the expected low thermal conductance and large temperature gradients along the length of the Baffle.
- The Strong-Box is modelled as 6 nodes, corresponding to the 4 side walls, the front wall (containing Vane 0) and the rear wall.

- The E-Box is modelled as 5 nodes, corresponding to the 4 side walls and the rear wall.
- The CCD Radiator is treated as a boundary node.
- The interface plate to which the Strong-Box was attached is also treated as a boundary node.

Several groups of nodes were assumed to be linked by high thermal conductances reflecting the fact that the components they represent are fabricated out of solid aluminium and that they are expected to be essentially isothermal. These are as follows:

- The 4 sides of each baffle section in the model are linked by conductances of 1.0 W/K since each of the real baffle sections is fabricated from solid aluminium, with a typical wall thickness of 1.5 mm.
- The side walls and rear wall of the Strong-Box are linked by conductances of 20 W/K since these are fabricated from a solid piece of aluminium, with wall thickness 5 mm. However, the front wall is a separate piece and the conductances between it and both the Strong-Box side walls to the rear, and the baffle stack to the front, were fitted as part of the model correlation.
- The side walls and rear wall of the E-Box are also linked by conductances of 20 W/K .

Conductive couplings which were fitted as part of the correlation of the model include:

- Conductance between each pair of sections along the length of the Baffle.
- Conductance between the rear section of the Baffle and the front wall of the Strong-Box.
- Conductance between the front wall of the Strong-Box and the side walls.
- Conductance between the Strong-Box and the E-Box.
- Conductance between the Strong-Box base and the spacecraft interface plate.

The MLI covering the instrument has not been modelled as a separate node but an effective emissivity of 0.02 has been assigned to the external surfaces of nodes to allow for its effect. An emissivity of 0.9 has been assumed for the internal surfaces of the Baffle (treated with Martin Black).

4. Test Set-Up

The thermal balance test was performed in a chamber which is approximately 1m diameter and 2.5m in length and is equipped with a cryogenic pump capable of maintaining the pressure below $1x10^{-6}$ mbar. A temperature-controlled table within the chamber can be set within the range -60 to +80°C.

The test configuration is shown in Figure 1. The Strong-Box was mounted onto the temperature-controlled table via a plate representative of the spacecraft interface, together with a thermal impedance of value 1.0 W/K which enabled the heat flow across the interface to be measured (by means of temperature sensors on either side of the impedance). Due to the limited space available inside the chamber the "flight-like" CCD Radiator on the Camera was removed and replaced by a radiator of a similar area (400 cm^2) which lay flat over the top of the Strong-Box. The Door was also removed for "Door Open" case tests.

To simulate the cooling due to space an L-shaped radiator (referred to below as the LN2 Radiator), which was cooled by means of a liquid nitrogen dewar and coldfinger assembly, was placed over the CCD Radiator and in front of the open aperture of the Baffle. Initially, a thermal impedance of value 0.2 W/K was installed between the liquid nitrogen dewar and the LN2 Radiator in order to measure the heat flow. However, this impedance was removed part-way through the tests in order to achieve more realistic temperatures at the LN2 Radiator (see Section 5).

A thermal impedance of value 0.6 W/K installed between the CCD Radiator and the CCD-Coldfinger assembly was used to measure the heat flow into the CCD Coldfinger.
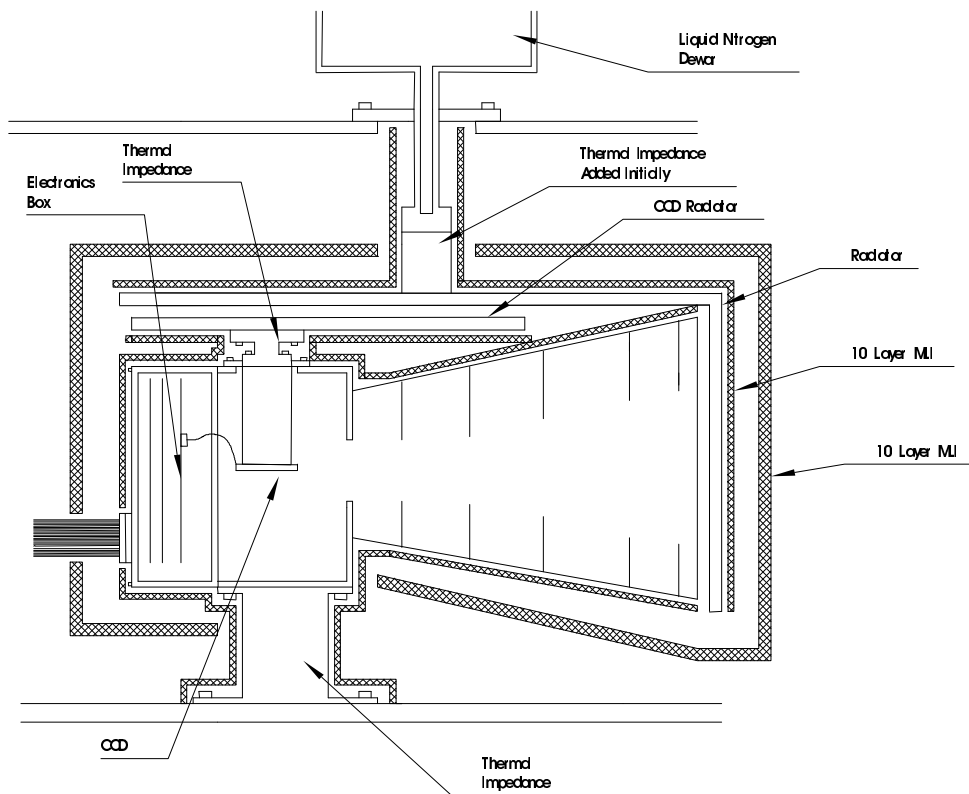
Figure 1 - A schematic diagram showing the SMEI thermal balance test set up.

A number of PRT100 temperature sensors were attached to the experimental set up. The locations of the PRTs on the camera itself were chosen to provide information about the interface temperature, the electronics temperature, and to enable the heat flow down the baffle to be modelled. The number and position of the PRTs on the Baffle was chosen carefully to provide the maximum information, but without causing the PRT harness to dominate the heat flow along the Baffle. The PRT allocations and locations are given in Table 2. The accuracy of the temperature sensors and data logging system is +/- 0.1 °C.

Heater mats were installed on the Baffle Front Section to simulate Solar UV or Earth IR input. It had been intended to simulate the actual in-orbit inputs predicted for Camera 3 in this way, but it was found that the cooling available from the LN2 dewar and coldfinger arrangement was somewhat limited and the maximum heater power which was applied in any test case was 10W. A heater mat installed on the CCD Coldfinger was used to investigate the effectiveness of the planned De-Icer Heaters in raising the CCD temperature in order to prevent contamination early in the mission.

As indicated in Figure 1, multi-layer insulation was installed first around the Camera itself, then around the outside of the LN2 Radiator and coldfinger, and finally over the whole assembly.

Interface cable harnesses were connected to the E-Box to allow the Camera electronics to be operated during the tests. The thermal conductivity along these harnesses was negligible. For the final five test cases (14-18) the E-Box was replaced by a mass dummy which had identical mechanical and thermal interfaces to the Strong-Box and had heaters to simulate the 6.3W dissipation of the FM Cameras.

PRT Channel	Location.
T00	E-Box
T01	Strong-Box
T02	Front wall of Strong-Box (Baffle Vane 0)
T03	Middle of Baffle (Baffle Vane 4)
T04	Rear end of Baffle (Baffle Vane 1)
T05	Front end of Baffle (Baffle Top Section)
T06	CCD Radiator end of thermal impedance (0.6 W/K)
T07	CCD Radiator (location 1)
T08	CCD Coldfinger end of thermal impedance (0.6 W/K)
T09	CCD Radiator (location 2)
T12	LN2 Radiator opposite CCD Radiator
T16	LN2 Radiator in front of Baffle
T18	Spacecraft interface: table end of thermal impedance (1.0 W/K).
T19	Spacecraft interface: Strong-Box end of thermal impedance (1.0 W/K).
T24	Radiator end of LN2 thermal impedance (0.2 W/K).
T25	Dewar end of LN2 thermal impedance (0.2 W/K).

Table 2 - Location of the PRT Temperature Sensors

5. Test Cases

In total 18 thermal test cases were carried out. The conditions in the tests are listed in Table 3.

Test Case	Table (°C)	Heater Power (W)			Door	Comments
		E-Box	CCD	Baffle		
1	-10.0	5.0	0.0	0.0	Open	
2	-10.0	5.0	0.0	10.0	"	
3	-10.0	5.0	5.0	0.0	"	
4	-10.0	5.0	10.0	0.0	"	
5	-10.0	5.0	0.0	5.0	"	
6	-10.0	0.0	0.0	0.0	"	
7	-20.0	0.0	0.0	0.0	"	
8	-20.0	5.0	0.0	0.0	"	
9	+30.0	5.0	0.0	0.0	"	
10	-10.0	5.0	0.0	0.0	"	Repeat of Test 1
11	-20.0	5.0	0.0	0.0	Closed	
12	-40.0	0.0	0.0	0.0	"	
13	-40.0	0.0	10.0	0.0	"	
14	-22.0	6.3	0.0	0.0	Open	
15	-28.0	0.0	0.0	0.0	"	SMEI Survival Mode
16	-33.0	0.0	10.0	0.0	"	De-icing in SMEI Survival Mode
17	-9.5	0.0	10.0	0.0	"	De-icing in SMEI Operating Mode
18	-14.5	6.3	0.0	0.0	"	SMEI Operating Mode

Table 3 - The Thermal Test Cases

The tests fell into two groups, the first being exploratory and the second were tests against which the thermal model was eventually correlated.

The aims of the exploratory tests were:

- To experimentally characterise the Camera.
- To identify the main heat flow paths.
- To quantify the total parasitic loads from the tank environment.
- To examine the effect of closing the Door.
- To obtain some preliminary measurements of the heater power requirements at the Strong-Box interface.

As described previously, three calibrated thermal impedances were used to measure heat flow along critical paths by means of a temperature sensor at each end of the impedance. The heat flows measured in this way were:

- Between the table and the Strong-Box spacecraft interface plate (using T18 and T19).
- Between the CCD-Coldfinger assembly and the CCD Radiator (using T8 and T6).
- Between the LN2 Radiator and the dewar (using T24 and T25).

Test cases 1-9 were carried out with the Door removed ("open" case). Test 10 was a repeat of Test 1 to check the repeatability of the experimental measurements. Tests 11-13 were carried out with the Door fitted (and closed).

These initial measurements were very useful in confirming that both the CCD-Coldfinger assembly and the Baffle system are very effectively de-coupled from the Strong-Box and camera electronics.

However, the main problem with the thermal impedances is that because of the temperature drops across them, the hardware experiences higher temperatures than desirable. This was especially true in the case of the LN2 Radiator whose temperature during some of the initial set of tests was as high as -70°C. This was considered to be too high since (a) it was unrepresentative of space and (b) the heat coupled back into the system from the cooling surfaces was too high a fraction of the net heat flux thus making it more difficult to model, particularly in the case of the Baffle.   In addition it was felt that with the baffles running warm, the differential expansion effects on the baffle assembly would lead to unrepresentative and different conductive couplings between the baffle elements. Furthermore, the temperature of the LN2 Radiator in different tests ranged from approximately -70°C to -160°C, depending on heat flows through the system. All these effects made correlation with a single model very difficult.

Consequently, the final five tests (Tests 14-18) against which the model was eventually correlated were carried out with the thermal impedance between the LN2 Radiator and the dewar removed. As a result the temperature of the LN2 Radiator was lower and much more consistent between the tests, ranging from approximately -160°C to -180°C. This also meant that extrapolations (to the space environment) of the measured power flows through the Strong-Box interface were less than previously and therefore less susceptible to error.

These final test cases were designed to simulate in-orbit operating conditions. The EM E-Box was removed and replaced by a mass dummy which had identical mechanical and thermal interfaces to the Strong-Box, and internal heaters to simulate the expected 6.3W dissipation of the FM electronics. In Tests 15 and 16 the temperature of the table was iteratively adjusted until the temperature at the Strong-Box interface (T19) was -32.5°C, corresponding to the SMEI Survival Mode specification of   -40°C minimum (assuming a 5°C design margin and spacecraft survival heaters cycling over a 5°C band). Similarly, in Tests 17 and 18 the temperature of the table was adjusted until the temperature at the Strong-Box interface was -12.5°C, corresponding to the SMEI Operating Mode specification of -20°C minimum.

6. Test Procedure

The outline test procedure is given in Appendix 2.

In each test case sufficient time was allowed for all temperatures to become stable to within $1°C$ per hour, and where possible to within $0.5°C$ per hour. This often required ≥ 12 hours.

For test cases 15-18 it was necessary to iteratively adjust the table temperature in order to achieve the required temperature at the Strong-Box spacecraft interface plate (T19).

7. Results

The results for the temperature sensor readings in the various test cases are given in Appendix 3.

Various aspects of the interpretation of the results are discussed in the following sections.

7.1 Initial Results for Conductive Links

An initial value for the conductance between the Strong-Box and the simulated spacecraft interface plate was derived directly from the temperature measurements, together with the known conductance of the thermal impedance in the support bracket, using the equation –

$$C = C_Z \times (T_{18} - T_{19}) / (T_{19} - T_{01})$$

where C_Z is the conductance of thermal impedance (1.0 W/K) and T_{01}, etc are the readings of the temperature sensors as defined in Table 2.

Test cases where the difference $(T_{19} - T_{01})$ was $\leq 0.2°C$ were rejected. The remaining cases gave a mean value of 6.7 W/K.

Similarly, an initial value for the conductance between the Strong-Box and the E-Box was derived directly from the temperature measurements, together with the known power dissipation in the E-Box (P_E), using the equation –

$$C = P_E / (T_{00} - T_{01})$$

Only cases where the EM E-Box was fitted and the Camera electronics was switched on were used. They gave a mean value of 2.3 W/K.

7.2 Parasitic Load on the CCD-Coldfinger Assembly

In a similar way the coupling between the CCD-Coldfinger assembly and the Strong-Box can be detemined directly from the temperature measurements. Assuming that the coupling is conductive in nature (or is represented by an equivalent conductance) then:

$$C = C_Z \times (T_{08} - T_{06}) / (T_{01} - T_{08})$$

where C_Z is the conductance of thermal impedance between the Coldfinger and the CCD Radiator (0.6 W/K) and T_{01}, etc are the readings of the temperature sensors as defined in Table 2.

The above equation is not valid for test cases where the CCD Heater is being used. Excluding these, the remainder of the test cases gave a mean value of 0.040 W/K.

However, it is to be expected that the coupling between the CCD-Coldfinger assembly and the Strong-Box will be partly conductive and partly radiative. If simple conductance values are calculated as above they will vary with temperature in the different test cases because of the radiative contribution. It was indeed found that there was a systematic variation of the derived conductance values with the typical temperatures in the system (Strong-Box and CCD).

A model including both the conductive and radiative components was then fitted to the results:

$$C_{MODEL} \approx C_{COND} + C_{RAD} \times T^3$$

where T is "mean" temperature of the system, i.e. the mean of the Strong-Box and CCD temperatures (T_{01} and T_{08}).

This model gave a significantly better fit to the data, the best fit being obtained with values for the coefficients of:

$$C_{COND} = 0.014 \quad W/K$$
$$C_{RAD} = 2 \times 10^{-9} \quad W/K^3$$

These values indicate that the conductive coupling constitutes about one third and the radiative coupling two thirds of the total.

However, over the fairly limited temperature range of interest the simple conductive coupling term with a conductance of 0.04 W/K represents the experimental results with errors of 10% or less. Consequently, we have used this in the thermal model correlation.

7.3 Heater Power Requirements

Test Case 14 was designed to simulate Survival Mode. As explained previously the table temperature was adjusted until the temperature at the Strong-Box spacecraft interface was -32.5°C, the expected mean temperature which will be maintained by the spacecraft survival heaters. At this temperature, and will no internal dissipation within the E-Box or Strong-Box, the measured power flowing across the interface is 5.8 W. Of course this is with the Baffle and CCD-Radiator viewing the LN2 Radiator at ~ 100°K. We estimate that the required power if the radiators are viewing 3°K will be ~ 6.3 W.

Similarly, Test Case 16 was designed to simulate Operating Mode. In this case the temperature at the spacecraft interface was -12.5°C, and the internal dissipation within the E-Box was 6.3 W. The measured power flowing across the interface is 0.7 W, which would increase to an estimated 1.3 W if the radiators are viewing 3°K.

7.4 Door Closed Tests

The main objective of the Test Cases with the Door fitted in the closed position (Test Cases 11-13) was to investigate the temperature of the Baffle Top Section under these conditions and compare it with the range of temperatures over which the HOP Actuator and Door Assembly was qualified in a recent thermal vacuum test in Birmingham. This range was -50°C to +60°C.

Even in worst-case Survival Mode conditions with no internal power dissipation in the Camera (Test Case 12) the temperature at the Baffle Top Section was -43°C, significantly above the thermal vacuum test cold case. With the Camera in Operating Mode (Test Case 11) the temperature was around -20°C.

(Even though it is not possible to have all 3 Cameras switched on during Door deployment, in order not to exceed the maximum power budget, there is no reason why the Camera whose door is actually being released should not be in Operating Mode and it is indeed desirable that this Camera should be switched on at this time).

7.5 Correlation with the Thermal Model

The thermal model was fitted to the five final test cases. As part of the fitting process the various conductive links were adjusted to optimise the agreement between model predictions and the measurements (see Section 7.5). The results of the correlation of the thermal model with these test cases are shown in Table 4. For each case the measured temperatures, the model predictions and the differences are given.

Test Case	Temp °C	E-Box (T0)	S-Box Body (T1)	S-Box I/F * (T19)	CCD * (T8)	S-Box Front (T2)	Baffle Rear (T4)	Baffle Middle (T3)	Baffle Front (T5)
14	Meas	-17.4	-18.9	-18.8	-79.9	-20.0	-58.2	-75.8	-85.6
	Pred	-17.2	-18.7	-18.8	-79.9	-19.9	-58.3	-74.1	-82.4
	Diff	-0.2	-0.2	N/A	N/A	-0.1	+0.1	-1.7	-3.2
15	Meas	-32.6	-32.8	-32.6	-86.6	-33.6	-67.6	-83.3	-92.2
	Pred	-33.1	-33.1	-32.6	-86.6	-34.2	-66.2	-79.9	-87.3
	Diff	+0.5	+0.3	N/A	N/A	+0.6	-1.4	-3.4	-4.9
16	Meas	-32.1	-32.3	-32.4	+3.4	-33.1	-65.2	-80.0	-89.0
	Pred	-32.4	-32.5	-32.4	+3.4	-33.5	-65.2	-78.7	-85.9
	Diff	+0.3	+0.2	N/A	N/A	+0.4	0.0	-1.3	-3.1
17	Meas	-12.8	-13.0	-12.9	+8.6	-13.9	-53.9	-72.8	-83.5
	Pred	-13.1	-13.1	-12.9	+8.6	-14.5	-54.5	-70.8	-79.3
	Diff	+0.3	+0.1	N/A	N/A	+0.6	+0.6	-2.0	-4.2
18	Meas	-11.2	-12.7	-12.5	-77.1	-13.8	-50.9	-69.3	-80.6
	Pred	-11.0	-12.4	-12.5	-77.1	-13.8	-54.7	-71.3	-80.0
	Diff	-0.2	-0.3	N/A	N/A	0.0	+3.8	+2.0	-0.6

* These are boundary nodes

Table 4 - Comparison Between Model Predictions and Measured Temperatures for Final Tests

It can be seen that the fits are better in the case of the Strong-Box and E-box than they are for the Baffle. The reasons for this are discussed below:

(i) The Strong-Box and E-Box

The agreements between test data and predictions are typically well within +/- 0.5°C. This is partly due to the fact that the heat coupling between these nodes is dominantly conductive and therefore modelling is more straightforward. In addition, since it is these elements which define the power drawn from the spacecraft interface (since the Baffle and CCD-Coldfinger are well de-coupled) the fitting of the model to these data has taken priority over the fitting to the Baffle data.

(ii) The Baffle

The modelling of the Baffle is complex because of (a) its design and construction, and (b) the parallel conductive and radiative transfer of heat along it. In order to keep the modelling tangible sufficient

nodes were required to be able to represent the expected temperature gradients and parallel heat paths but without causing the number of heat couplings to be excessive. Consequently, the baffle representation is not likely to be as realistic as that of the other elements.

However, the correlations match the front-to-back gradients to within 10%, although the correlations with the individual nodes of the baffle are not always as good as that. Bearing in mind that both the model and the measurements demonstrate the insulating effects of the baffle it was not seen as a high priority to improve the modelling which may well have required more nodes to represent the seven separate elements of the baffle. Another concern relates to differential expansion changing the values of the conductive links (though the repeatability of the tests was demonstrated).

7.6 Thermal Conductivity along the Baffle Assembly

A major objective of the tests was to derive values for the thermal conductances along the Baffle, and between the Baffle and the Strong-Box (initially these values were very uncertain). Using the model node definitions as described previously (see Section 3) the values obtained as a result of correlating the thermal model are given in Table 5.

Conductive Couplings	Conductance (W/K)	
	Per Node	Total
Baffle Front to Middle Section (e.g. Nodes 3-2)	0.050	0.20
Baffle Middle to Rear Section (e.g. Nodes 2-1)	0.033	0.13
Baffle Rear to Strong-Box Front Plate (e.g. Nodes 1-13)	0.020	0.08
Strong-Box Front Plate to Side Walls (e.g. Nodes 13-15)	0.600	2.40

Table 5 - Results for Conductive Couplings along the Baffle Assembly

8. Conclusions

The following major objectives of the thermal balance tests have been achieved:

- To demonstrate that the Baffle assembly is thermally de-coupled from the Strong-Box, and to determine the relevant thermal conductivities.
- To demonstrate that the CCD-Coldfinger assembly is also thermally de-coupled from the Strong-Box, and to determine the parasitic thermal load on the CCD.
- To obtain an initial estimate for the heater power required at the Strong-Box spacecraft interface to maintain the Camera within the survival temperature range when it is unpowered.
- To correlate the SMEI Camera thermal model against the measurements.

The correlation has been carried out using the five final test cases and the model is well correlated within the required accuracies.

Test cases with the Door closed demonstrated that in cold cases the temperature at the Baffle Top Section will be within the range over which the HOP Actuator and Door system has been qualified in a recent thermal vacuum test. A more serious concern is the hot case in respect of Camera 3, where there is a substantial Solar UV flux incident on the Baffle, which must be provided with radiating surfaces so that its temperature is safely below the +60°C hot case temperature at which the Door system has been qualified (the melting point of the paraffin wax in the HOP is +70°C). This problem will need to be addressed by thermal modelling, and possibly in future thermal testing.

The tests have not been so useful in terms of determining the expected CCD operating temperatures. It can be seen from Appendix 3 that the CCD temperatures (T08) ranged from approximately -40°C to -80°C in the different test cases, well below the design requirement of -30°C. However, there are two significant respects in which the thermal balance test conditions differed from the in-orbit situation.

Firstly, the CCD Radiator was viewing the LN2 radiator whose temperature was considerably above that of "deep space". On the other hand, the view factor in the tests was close to unity, whereas the view factors to space of the Radiators when the Cameras are mounted on the spacecraft are typically ~0.75, with the remaining ~0.25 being to SMEI and spacecraft MLI. Consequently, the determination of in-orbit CCD operating temperatures depends on integration of the SMEI Camera thermal model into a model of the entire spacecraft.

The correlated thermal model now has to be used to complete the following tasks:

- To determine the in-orbit quasi steady state temperatures using average Solar UV and Earth IR fluxes, together with the local spacecraft environment.
- To determine the orbital variations of these temperatures.
- To confirm that the provisionally selected radiator orientations (all rotated by 45°) give acceptable CCD temperatures for all three cameras in all thermal cases.
- To reduce the active area of the radiators to still allow sufficient cooling of the CCDs whilst achieving the highest temperatures with the available De-Icer Heater powers.
- To produce final power inputs at the spacecraft interface to maintain the required temperature of the interface under these new conditions.

Since all the above depend significantly on the local spacecraft environment (view factors and temperatures) they are best investigated using an integrated spacecraft thermal model.

_____

Appendix 1

Diagrams Showing Nodes in SMEI Thermal Model

THERMICA
16-Nov-1999 18:85:48
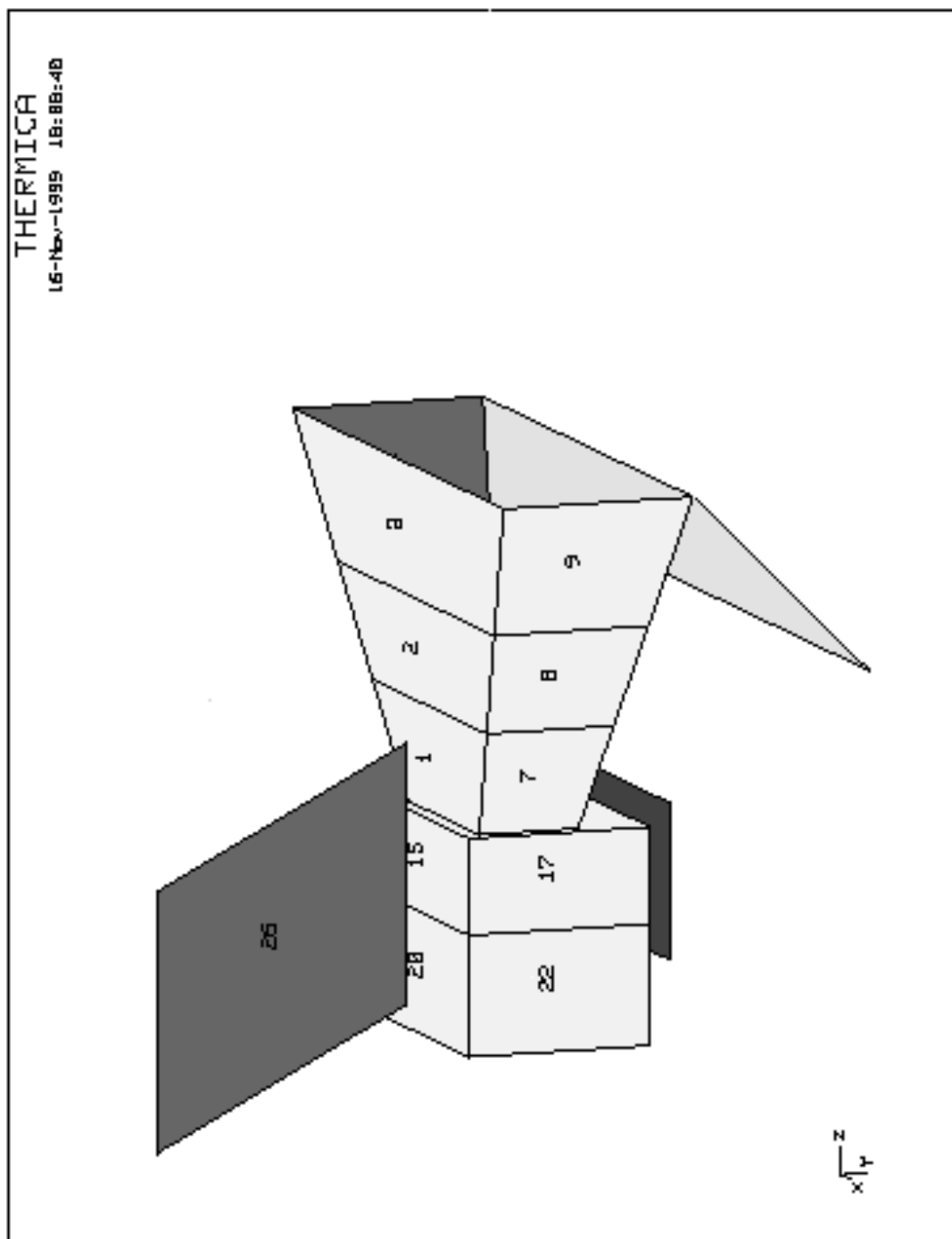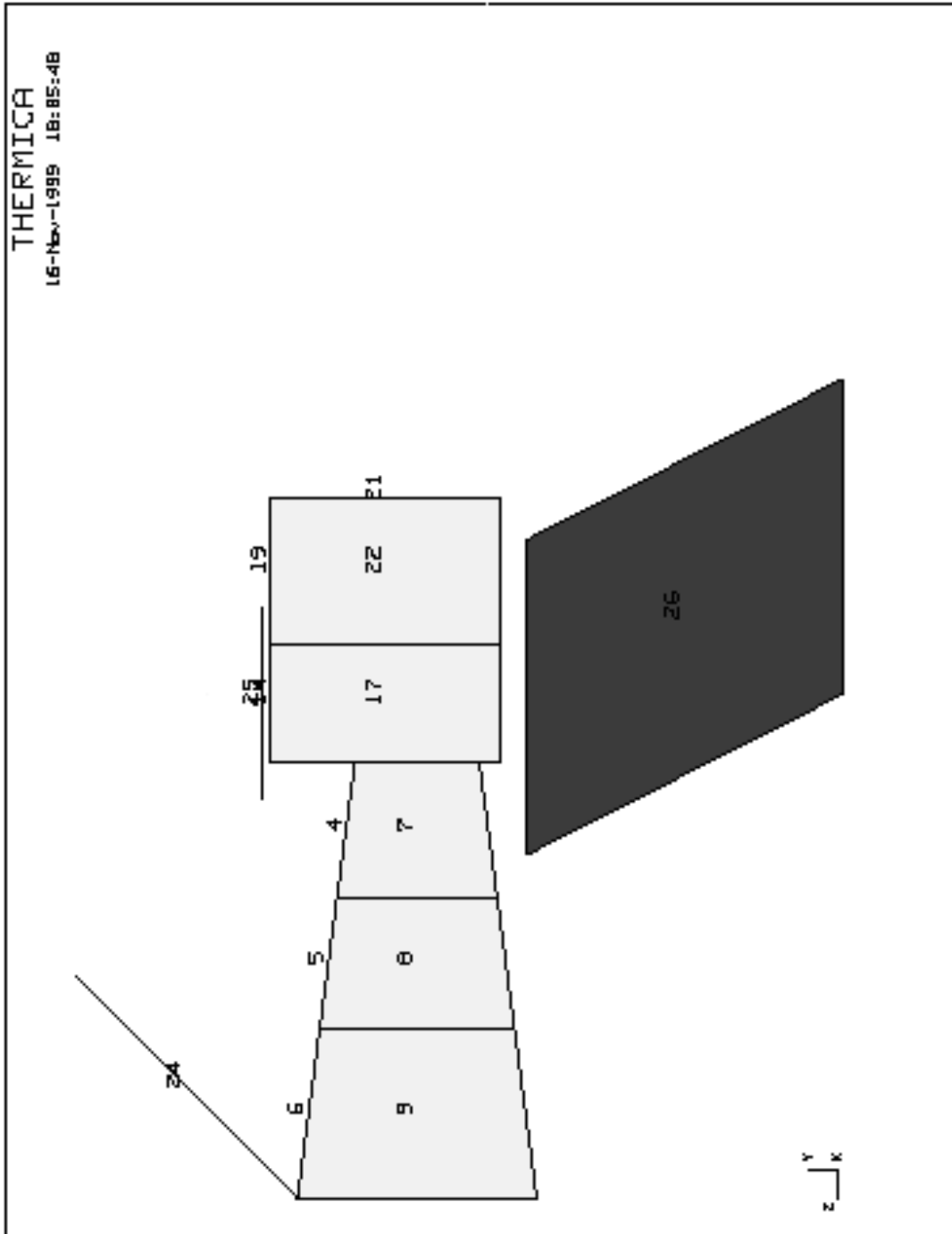
Appendix 2

Outline Test Procedure

A. Initial Configuration

- Door removed (i.e. "open").
- Thermal impedance (0.2 W/K) installed between the liquid nitrogen dewar and the LN2 Radiator.

1. Pump down to $<10^{-5}$ mbar.
2. Cool dewar and LN2 Radiator.
3. Set table to -10°C.
4. Switch on Camera electronics (5W).
5. Wait for all temperatures stable to < 1°C per hour.
6. Record temperatures (Test Case 1).
7. Switch on Baffle Heater at 10W.
8. Wait for all temperatures stable to < 1°C per hour.
9. Record temperatures (Test Case 2).
10. Switch off Baffle Heater and switch on CCD-Coldfinger Heater at 5W.
11. Wait for all temperatures stable to < 1°C per hour.
12. Record temperatures (Test Case 3).
13. Switch on CCD-Coldfinger Heater at 10W.
14. Wait for all temperatures stable to < 1°C per hour.
15. Record temperatures (Test Case 4).
16. Switch off CCD-Coldfinger Heater and switch on Baffle Heater at 5W.
17. Wait for all temperatures stable to < 1°C per hour.
18. Record temperatures (Test Case 5).
19. Switch off all heaters and Camera electronics.
20. Wait for all temperatures stable to < 1°C per hour.
21. Record temperatures (Test Case 6).
22. Set table to -20°C.
23. Wait for all temperatures stable to < 1°C per hour.
24. Record temperatures (Test Case 7).
25. Switch on Camera electronics (5W).
26. Wait for all temperatures stable to < 1°C per hour.
27. Record temperatures (Test Case 8).
28. Set table to +30°C.
29. Wait for all temperatures stable to < 1°C per hour.
30. Record temperatures (Test Case 9).
31. Set table to -10°C.
32. Wait for all temperatures stable to < 1°C per hour.
33. Record temperatures (Test Case 10).
34. Set table to +30°C.
35. Warm up dewar and LN2 Radiator.
36. Wait for all temperatures > +15°C.
37. Switch off Camera electronics.
38. Bring tank up to air.

B. Door Closed Cases

- Door fitted in closed configuration.
- Thermal impedance (0.2 W/K) installed between the liquid nitrogen dewar and the LN2 Radiator.

1. Pump down to $<10^{-5}$ mbar.
2. Cool dewar and LN2 Radiator.
3. Set table to -20°C.
4. Switch on Camera electronics (5W).
5. Wait for all temperatures stable to < 1°C per hour.
6. Record temperatures (Test Case 11).
7. Set table to -40°C.
8. Switch off Camera electronics
9. Wait for all temperatures stable to < 1°C per hour.
10. Record temperatures (Test Case 12).
11. Switch on CCD-Coldfinger Heater at 10W.
12. Wait for all temperatures stable to < 1°C per hour.
13. Record temperatures (Test Case 13).
14. Set table to +30°C.
15. Warm up dewar and LN2 Radiator.
16. Wait for all temperatures > +15°C.
17. Switch off Camera electronics.
18. Bring tank up to air.

C. Final Tests

- Door removed (i.e. "open").
- Thermal impedance (0.2 W/K) between the liquid nitrogen dewar and the LN2 Radiator *removed*.
- E-box removed and replaced by mass dummy with 6.3W heater.

1. Pump down to $<10^{-5}$ mbar.
2. Cool dewar and LN2 Radiator.
3. Set table to -22°C.
4. Switch on E-box Heater (6.3W).
5. Wait for all temperatures stable to < 1°C per hour.
6. Record temperatures (Test Case 14).
7. Set table to -30°C.
8. Switch off E-box Heater.
9. Adjust table temperature until Spacecraft Interface temperature (T19) is -32.5+/-0.5°C.
10. Wait for all temperatures stable to < 1°C per hour.
11. Record temperatures (Test Case 15 – SMEI Survival Mode).
12. Switch on CCD-Coldfinger Heater at 10W.
13. Adjust table temperature until Spacecraft Interface temperature (T19) is -32.5+/-0.5°C.
14. Wait for all temperatures stable to < 1°C per hour.
15. Record temperatures (Test Case 16 – De-icing in SMEI Survival Mode).
16. Adjust table temperature until Spacecraft Interface temperature (T19) is -12.5+/-0.5°C.
17. Record temperatures (Test Case 17 – De-icing in SMEI Operating Mode).
18. Switch off CCD-Coldfinger Heater and switch on E-box Heater (6.3W).
19. Adjust table temperature until Spacecraft Interface temperature (T19) is -12.5+/-0.5°C.
20. Wait for all temperatures stable to < 1°C per hour.
21. Record temperatures (Test Case 18 – SMEI Operating Mode).
22. Set table to +30°C.
23. Warm up dewar and LN2 Radiator.
24. Wait for all temperatures > +15°C.
25. Switch off E-box Heater
26. Bring tank up to air.

Appendix 3

Results for Temperature Sensor Readings in the Test Cases

Test Case	Temperature Sensor Readings															
	T00	T01	T02	T03	T04	T05	T06	T07	T08	T09	T12	T16	T18	T19	T24	T25
1	-7.7	-9.9	-11.1	-53.9	-40.2	-61.4	-64.9	-65.3	-61.4	-65.7	-115.4	-109.7	-7.9	-9.7	-117.4	-162.1
2	-2.6	-4.5	-5.1	-9.0	-8.3	-5.2	-48.4	-48.8	-45.4	-49.2	-77.0	-64.3	-6.7	-4.8	-78.7	-146.1
3	-6.0	-8.1	-9.2	-43.2	-31.9	-50.6	-22.7	-24.3	-13.7	-25.4	-91.2	-87.5	-7.9	-7.3	-94.7	-148.4
4	-3.2	-5.2	-6.2	-34.2	-24.6	-40.8	+7.0	+4.3	+21.7	+2.6	-70.0	-68.5	-6.8	-5.2	-75.1	-138.0
5	-5.1	-7.1	-8.0	-24.1	-19.0	-18.9	-52.7	-53.1	-49.6	-53.5	-85.0	-80.4	-7.3	-7.0	-88.4	-145.2
6	-15.3	-15.9	-16.8	-54.0	-42.1	-61.4	-67.1	-67.5	-63.9	-67.8	-114.2	-108.4	-9.3	-15.5	-116.0	-159.2
7	-23.5	-24.2	-25.1	-60.7	-49.3	-67.6	-72.2	-72.6	-69.3	-72.9	-121.1	-115.7	-18.7	-23.9	-122.8	-164.2
8	-16.4	-18.7	-19.8	-60.6	-48.3	-67.9	-70.9	-71.3	-67.7	-71.6	-121.8	-116.7	-17.2	-18.4	-123.6	-163.7
9	+24.2	+22.2	+20.9	-25.0	-8.4	-36.1	-45.6	-46.3	-40.5	-47.0	-93.9	-87.2	+29.5	+22.8	-98.2	-159.8
10	-8.0	-10.2	-11.4	-53.2	-39.8	-61.3	-66.8	-67.2	-63.5	-67.5	-114.8	-109.7	-8.0	-9.9	-116.6	-159.0
11	-12.3	-14.1	-14.6	-18.4	-17.3	-19.5	-74.8	-75.2	-71.1	-75.6	-152.5	-152.0	-16.4	-14.1	-154.9	-182.6
12	-38.1	-38.4	-38.8	-42.0	-41.1	-42.7	-87.6	-87.9	-84.8	-88.1	-160.8	-160.5	-37.2	-38.4	-162.7	-184.7
13	-33.7	-33.8	-34.2	-37.5	-36.4	-38.4	-8.2	-10.8	+6.2	-12.5	-120.8	-124.9	-36.1	-34.1	-126.8	-174.0
14	-17.4	-18.9	-20.0	-75.8	-58.2	-85.6	-83.2	-83.6	-79.9	-83.9	-176.5	-171.2	-19.0	-18.8	N/A	N/A
15	-32.6	-32.8	-33.6	-83.3	-67.6	-92.2	-89.5	-89.8	-86.6	-90.0	-178.5	-174.0	-26.8	-32.6	N/A	N/A
16	-32.1	-32.3	-33.1	-80.0	-65.2	-89.0	-11.4	-14.0	+3.4	-15.7	-164.1	-163.6	-30.5	-32.4	N/A	N/A
17	-12.8	-13.0	-13.9	-72.8	-53.9	-83.5	-7.2	-10.0	+8.6	-11.8	-162.0	-161.0	-8.2	-12.9	N/A	N/A
18	-11.2	-12.7	-13.8	-69.3	-50.9	-80.6	-80.7	-81.1	-77.1	-81.4	-174.8	-168.7	-11.8	-12.5	N/A	N/A

Appendix 4

Listings of Thermal Model

The following is a listing of the ESATAN/THERMICA file defining the thermal nodes and their surface properties as used in the correlation with the thermal balance tests:

```
$DATA   UNIT=MM  SPACE=10000

<1> Lower Baffle -1
  $INFO COLOUR=BLUE
  $TSHAPE
  POINT/PP15   (-78.2,-39.5,0.00)
  POINT/PP16   (78.2,-39.5,0.00)
  POINT/PP19   (-125.73,-50.78,85.78)
  POINT/PP20   (125.73,-50.78,85.78)
  QUADRANGLE  P1=PP20 P2=PP16 P3=PP15 P4=PP19
  TMESH  SIDE=BOTH
  $THERMAL ALPHA=(0.9,0.02) EPSILON=(0.90,0.02) SPECA=(0.1,1)  NAME=(1)

<2> Lower Baffle -2
  $INFO COLOUR=BLUE
  $TSHAPE
  POINT/PP19   (-125.73,-50.78,85.78)
  POINT/PP20   (125.73,-50.78,85.78)
  POINT/PP23   (-171.87,-61.73,169.04)
  POINT/PP24   (171.87,-61.73,169.04)
  QUADRANGLE  P1=PP24 P2=PP20 P3=PP19 P4=PP23
  TMESH  SIDE=BOTH
  $THERMAL ALPHA=(0.9,0.02) EPSILON=(0.90,0.02) SPECA=(0.1,1)  NAME=(2)

<3> Lower Baffle -3
  $INFO COLOUR=BLUE
  $TSHAPE
  POINT/PP23   (-171.87,-61.73,169.04)
  POINT/PP24   (171.87,-61.73,169.04)
  POINT/PP27   (-231.57,-75.90,276.80)
  POINT/PP28   (231.57,-75.90,276.80)
  QUADRANGLE  P1=PP28 P2=PP24 P3=PP23 P4=PP27
  TMESH  SIDE=BOTH
  $THERMAL ALPHA=(0.9,0.02) EPSILON=(0.90,0.02) SPECA=(0.1,1)  NAME=(3)

<4> Top Baffle -1
  $INFO COLOUR=BLUE
  $TSHAPE
  POINT/PP13   (78.2,39.5,0.00)
  POINT/PP14   (-78.2,39.5,0.00)
  POINT/PP17   (125.73,50.78,85.78)
  POINT/PP18   (-125.73,50.78,85.78)
  QUADRANGLE  P1=PP17 P2=PP18 P3=PP14 P4=PP13
  TMESH  SIDE=BOTH
  $THERMAL ALPHA=(0.9,0.02) EPSILON=(0.90,0.02) SPECA=(0.1,1)  NAME=(4)

<5> Top Baffle -5
  $INFO COLOUR=BLUE
  $TSHAPE
  POINT/PP17   (125.73,50.78,85.78)
```

```
   POINT/PP18   (-125.73,50.78,85.78)
   POINT/PP21   (171.87,61.73,169.04)
   POINT/PP22   (-171.87,61.73,169.04)
   QUADRANGLE  P1=PP21  P2=PP22  P3=PP18  P4=PP17
   TMESH  SIDE=BOTH
  $THERMAL ALPHA=(0.9,0.02) EPSILON=(0.90,0.02) SPECA=(0.1,1)  NAME=(5)


<6> Top Baffle -6
   $INFO COLOUR=BLUE
   $TSHAPE
   POINT/PP21   (171.87,61.73,169.04)
   POINT/PP22   (-171.87,61.73,169.04)
   POINT/PP25   (231.57,75.90,276.80)
   POINT/PP26   (-231.57,75.90,276.80)
   QUADRANGLE  P1=PP25  P2=PP26  P3=PP22  P4=PP21
   TMESH  SIDE=BOTH
  $THERMAL ALPHA=(0.9,0.02) EPSILON=(0.90,0.02) SPECA=(0.1,1)  NAME=(6)


<7> Right  Baffle -1
   $INFO COLOUR=BLUE
   $TSHAPE
   POINT/PP13   (78.2,39.5,0.00)
   POINT/PP16   (78.2,-39.5,0.00)
   POINT/PP17   (125.73,50.78,85.78)
   POINT/PP20   (125.73,-50.78,85.78)
   QUADRANGLE  P1=PP20  P2=PP17  P3=PP13  P4=PP16
   TMESH  SIDE=BOTH
  $THERMAL ALPHA=(0.9,0.02) EPSILON=(0.9,0.02) SPECA=(0.1,1)  NAME=(7)


<8> Right Baffle -2
   $INFO COLOUR=BLUE
   $TSHAPE
   POINT/PP17   (125.73,50.78,85.78)
   POINT/PP20   (125.73,-50.78,85.78)
   POINT/PP21   (171.87,61.73,169.04)
   POINT/PP24   (171.87,-61.73,169.04)
   QUADRANGLE  P1=PP24  P2=PP21  P3=PP17  P4=PP20
   TMESH  SIDE=BOTH
  $THERMAL ALPHA=(0.9,0.02) EPSILON=(0.9,0.02) SPECA=(0.1,1)  NAME=(8)


<9> Right Baffle -3
   $INFO COLOUR=BLUE
   $TSHAPE
   POINT/PP21   (171.87,61.73,169.04)
   POINT/PP24   (171.87,-61.73,169.04)
   POINT/PP25   (231.57,75.90,276.80)
   POINT/PP28   (231.57,-75.90,276.80)
   QUADRANGLE  P1=PP28  P2=PP25  P3=PP21  P4=PP24
   TMESH  SIDE=BOTH
  $THERMAL ALPHA=(0.9,0.02) EPSILON=(0.90,0.02) SPECA=(0.1,1)  NAME=(9)


<10>Left Baffle -1
   $INFO COLOUR=BLUE
   $TSHAPE
   POINT/PP14   (-78.2,39.5,0.00)
   POINT/PP15   (-78.2,-39.5,0.00)
   POINT/PP18   (-125.73,50.78,85.78)
   POINT/PP19   (-125.73,-50.78,85.78)
   QUADRANGLE  P1=PP19  P2=PP15  P3=PP14  P4=PP18
   TMESH  SIDE=BOTH
  $THERMAL ALPHA=(0.9,0.02) EPSILON=(0.9,0.02) SPECA=(0.1,1)  NAME=(10)
```

<11> Left Baffle -2
  $INFO COLOUR=BLUE
  $TSHAPE
  POINT/PP18 (-125.73,50.78,85.78)
  POINT/PP19 (-125.73,-50.78,85.78)
  POINT/PP22 (-171.87,61.73,169.04)
  POINT/PP23 (-171.87,-61.73,169.04)
  QUADRANGLE P1=PP23 P2=PP19 P3=PP18 P4=PP22
  TMESH SIDE=BOTH
  $THERMAL ALPHA=(0.9,0.02) EPSILON=(0.9,0.02) SPECA=(0.1,1) NAME=(11)

<12> Left Baffle -3
  $INFO COLOUR=BLUE
  $TSHAPE
  POINT/PP22 (-171.87,61.73,169.04)
  POINT/PP23 (-171.87,-61.73,169.04)
  POINT/PP26 (-231.57,75.90,276.80)
  POINT/PP27 (-231.57,-75.90,276.80)
  QUADRANGLE P1=PP27 P2=PP23 P3=PP22 P4=PP26
  TMESH SIDE=BOTH
  $THERMAL ALPHA=(0.9,0.02) EPSILON=(0.90,0.02) SPECA=(0.1,1) NAME=(12)

<13> Front Strong Box
  $INFO COLOUR=BLUE
  $TSHAPE
  POINT/PP9   (91.0,93.0,0.00)
  POINT/PP10 (-91.0,93.0,0.00)
  POINT/PP11 (-91.0,-52.4,0.00)
  POINT/PP12 (91.0,-52.4,0.00)
  QUADRANGLE P1=PP11 P2=PP10 P3=PP9 P4=PP12
  TMESH SIDE=BOTH
  $THERMAL ALPHA=(0.2,0.02) EPSILON=(0.4,0.02) SPECA=(0.1,1) NAME=(13)

<14> Top Strong Box
  $INFO COLOUR=BLUE
  $TSHAPE
  POINT/PP5   (90.90,92.90,-74.00)
  POINT/PP6   (-90.90,92.90,-74.00)
  POINT/PP9   (91.0,93.0,0.00)
  POINT/PP10 (-91.0,93.0,0.00)
  QUADRANGLE P1=PP5 P2=PP9 P3=PP10 P4=PP6
  TMESH SIDE=BOTH
  $THERMAL ALPHA=(0.2,0.02) EPSILON=(0.4,0.02) SPECA=(0.1,1) NAME=(14)

<15> Base Strong Box
  $INFO COLOUR=BLUE
  $TSHAPE
  POINT/PP7   (-90.90,-52.40,-74.00)
  POINT/PP8   (90.90,-52.40,-74.00)
  POINT/PP11 (-91.0,-52.4,0.00)
  POINT/PP12 (91.0,-52.4,0.00)
  QUADRANGLE P1=PP8 P2=PP7 P3=PP11 P4=PP12
  TMESH SIDE=BOTH
  $THERMAL ALPHA=(0.2,0.02) EPSILON=(0.4,0.02) SPECA=(0.1,1) NAME=(15)

<16> Back Face Strong Box
  $INFO COLOUR=BLUE
  $TSHAPE
  POINT/PP5   (90.90,92.90,-74.00)
  POINT/PP6   (-90.90,92.90,-74.00)

```
  POINT/PP7   (-90.90,-52.40,-74.00)
  POINT/PP8   (90.90,-52.40,-74.00)
  QUADRANGLE  P1=PP7  P2=PP8  P3=PP5  P4=PP6
  TMESH  SIDE=BOTH
 $THERMAL ALPHA=(0.2,0.02) EPSILON=(0.4,0.02) SPECA=(0.1,1)  NAME=(16)


<17> Right Side Strong Box
  $INFO COLOUR=BLUE
  $TSHAPE
  POINT/PP5   (90.90,92.90,-74.00)
  POINT/PP8   (90.90,-52.40,-74.00)
  POINT/PP9   (91.0,93.0,0.00)
  POINT/PP12  (91.0,-52.4,0.00)
  QUADRANGLE  P1=PP12  P2=PP9  P3=PP5  P4=PP8
  TMESH  SIDE=BOTH
 $THERMAL ALPHA=(0.2,0.02) EPSILON=(0.4,0.02) SPECA=(0.1,1)  NAME=(17)


<18> Left Side Strong Box
  $INFO COLOUR=BLUE
  $TSHAPE
  POINT/PP6   (-90.90,92.90,-74.00)
  POINT/PP7   (-90.90,-52.40,-74.00)
  POINT/PP10  (-91.0,93.0,0.00)
  POINT/PP11  (-91.0,-52.4,0.00)
  QUADRANGLE  P1=PP11  P2=PP7  P3=PP6  P4=PP10
  TMESH  SIDE=BOTH
 $THERMAL ALPHA=(0.2,0.02) EPSILON=(0.4,0.02) SPECA=(0.1,1)  NAME=(18)


<19> Top E. Box
  $INFO COLOUR=BLUE
  $TSHAPE
  POINT/PP1   (90.90,92.90,-167.00)
  POINT/PP2   (-90.90,92.90,-167.00)
  POINT/PP5   (90.90,92.90,-74.00)
  POINT/PP6   (-90.90,92.90,-74.00)
  QUADRANGLE  P1=PP1  P2=PP5  P3=PP6  P4=PP2
  TMESH  SIDE=BOTH
 $THERMAL ALPHA=(0.2,0.02) EPSILON=(0.4,0.02) SPECA=(0.1,1)  NAME=(19)


<20> Base E. Box
  $INFO COLOUR=BLUE
  $TSHAPE
  POINT/PP3   (-90.90,-52.40,-167.00)
  POINT/PP4   (90.90,-52.40,-167.00)
  POINT/PP7   (-90.90,-52.40,-74.00)
  POINT/PP8   (90.90,-52.40,-74.00)
  QUADRANGLE  P1=PP8  P2=PP4  P3=PP3  P4=PP7
  TMESH  SIDE=BOTH
 $THERMAL ALPHA=(0.2,0.02) EPSILON=(0.4,0.02) SPECA=(0.1,1)  NAME=(20)


<21> Back E. Box
  $INFO COLOUR=BLUE
  $TSHAPE
  POINT/PP1   (90.90,92.90,-167.00)
  POINT/PP2   (-90.90,92.90,-167.00)
  POINT/PP3   (-90.90,-52.40,-167.00)
  POINT/PP4   (90.90,-52.40,-167.00)
  QUADRANGLE  P1=PP1  P2=PP2  P3=PP3  P4=PP4
  TMESH  SIDE=BOTH
 $THERMAL ALPHA=(0.2,0.02) EPSILON=(0.4,0.02) SPECA=(0.1,1)  NAME=(21)
```

<22> Right Side E. Box
  $INFO COLOUR=BLUE
  $TSHAPE
  POINT/PP1   (90.90,92.90,-167.00)
  POINT/PP4   (90.90,-52.40,-167.00)
  POINT/PP5   (90.90,92.90,-74.00)
  POINT/PP8   (90.90,-52.40,-74.00)
  QUADRANGLE P1=PP8 P2=PP5 P3=PP1 P4=PP4
  TMESH SIDE=BOTH
  $THERMAL ALPHA=(0.2,0.02) EPSILON=(0.4,0.02) SPECA=(0.1,1) NAME=(22)

<23> Left Side E. Box
  $INFO COLOUR=BLUE
  $TSHAPE
  POINT/PP2   (-90.90,92.90,-167.00)
  POINT/PP3   (-90.90,-52.40,-167.00)
  POINT/PP6   (-90.90,92.90,-74.00)
  POINT/PP7   (-90.90,-52.40,-74.00)
  QUADRANGLE P1=PP7 P2=PP3 P3=PP2 P4=PP6
  TMESH SIDE=BOTH
  $THERMAL ALPHA=(0.2,0.02) EPSILON=(0.4,0.02) SPECA=(0.1,1) NAME=(23)

<24> Door   *(Note: This node is not used in correlation with thermal balance test)*
  $INFO COLOUR=GREEN
  $TSHAPE
  POINT/PP25   (231.57,75.90,276.80)
  POINT/PP26   (-231.57,75.90,276.80)
  POINT/PP29   (231.57,217.60,135.09)
  POINT/PP30   (-231.57,217.60,135.09)
  QUADRANGLE P1=PP25 P2=PP29 P3=PP30 P4=PP26
  TMESH SIDE=BOTH
  $THERMAL ALPHA=(0.2,0.02) EPSILON=(0.02,0.02) SPECA=(0.1,0.1) NAME=(24)

<25> Base Plate
  $INFO COLOUR=YELLOW
  $TSHAPE
  POINT/PP35   (120.0,98.0,-97.0)
  POINT/PP36   (-120.0,98.0,-97.0)
  POINT/PP37   (-120.0,98.0,23.0)
  POINT/PP38   (120.0,98.0,23.0)
  QUADRANGLE P1=PP35 P2=PP36 P3=PP37 P4=PP38
  TMESH SIDE=BOTH
  $THERMAL ALPHA=(0.02,0.02) EPSILON=(0.02,0.02) SPECA=(0.1,0.1) NAME=(25)

<26> Radiator
  $INFO COLOUR=BLUE
  $TSHAPE
  POINT/PP43   (0.0,-69.50,-141.0)
  POINT/PP44   (0.0,-69.50,59.0)
  POINT/PP45   (0.0,-269.50,-42.91)
  POINT/PP46   (0.0,-269.50,-242.91)
  QUADRANGLE P1=PP43 P2=PP44 P3=PP45 P4=PP46
  TMESH SIDE=BOTH
  $THERMAL ALPHA=(0.9,0.02) EPSILON=(0.9,0.02) SPECA=(0.1,1) NAME=(26)

  $END

The following is a listing of the ESATAN/THERMICA file defining the conductive couplings between the
thermal nodes as used in the correlation with the thermal balance tests:

```
#  SMEI THERMAL MODEL - CONDUCTIVE COUPLLINGS
#
GL (1, 2) =  0.0330;
GL (1, 7) = 1.00;
GL (1, 10) = 1.00;
#
GL (2, 3) = 0.050;
GL (2, 8) = 1.00;
GL (2, 11) = 1.00;
#
GL (3, 9) = 1.00;
GL (3, 12) = 1.00;
#
GL (4, 5) = 0.0330;
GL (4, 7) = 1.00;
GL (4, 10) = 1.00;
#
GL (5, 6) = 0.050;
GL (5, 8) = 1.00;
GL (5, 11) = 1.00;
#
GL (6, 9) = 1.00;
GL (6, 12) = 1.00;
#
GL (7, 8) = 0.0330;
#
GL (8, 9) = 0.050;
#
GL (10, 11) = 0.0330;
#
GL (11, 12) = 0.050;
#
#
GL (14, 16) = 20.0;
GL (14, 17) = 20.0;
GL (14, 18) = 20.0;
GL (14, 19) = 1.050;
#
GL (15, 16) = 20.0;
GL (15, 17) = 20.0;
GL (15, 18) = 20.0;
GL (15, 20) = 1.050;
#
GL (16, 17) = 20.0;
GL (16, 18) = 20.0;
#
GL (16, 19) = 0.05;
GL (16, 20) = 0.05;
GL (16, 22) = 0.05;
GL (16, 23) = 0.05;
#
GL (17, 22) = 1.050;
#
GL (18, 23) = 1.050;
#


GL (19, 21) = 20.0;
GL (19, 22) = 20.0;
GL (19, 23) = 20.0;
```

```
#
GL (20, 21) = 20.0;
GL (20, 22) = 20.0;
GL (20, 23) = 20.0;
#
GL (21, 22) = 20.0;
GL (21, 23) = 20.0;
#
# ----------------- FRONT S.BOX TO BAFFLE
#
GL (1, 13) = 0.020;
GL (4, 13) = 0.020;
GL (7, 13) = 0.020;
GL (10, 13) = 0.020;
#
# ----------------- FRONT S.BOX TO S.BOX
#
GL (13, 14) = 0.60;
GL (13, 15) = 0.60;
GL (13, 17) = 0.60;
GL (13, 18)  =0.60;
#
# ----------------- Nodes 25 and 26 are BOUNDARY NODES
#
GL (25, 14) = 9.00;
GL (26,15) = 0.04;
```

_____